Estimating Juvenile Recruitment of Elk in an Occupancy Modeling Framework

By
Mateen Hessami

Undergraduate Thesis
Wildlife Biology Program
University of Montana
Missoula, MT

May 2018

Approved by:
Committee Chair: Dr. Mark Hebblewhite
Wildlife Biology Program
Department of Ecosystem and Conservation Sciences
W.A. Franke College of Forestry and Conservation
University of Montana

Dr. Mike Mitchell
Wildlife Biology Program
Montana Cooperative Wildlife Research Unit,
University of Montana

Dr. Joshua Nowak
Wildlife Biology Program
W.A. Franke College of Forestry and Conservation
University of Montana

Jesse Whittington
Parks Canada, Banff Field Unit

Mateen Hessami, B.S., Spring 2019
Estimating Juvenile Recruitment of Elk in an Occupancy Framework

Chairperson: Mark Hebblewhite

ABSTRACT

Juvenile recruitment is a key parameter in understanding ungulate population dynamics. Traditional methods in population composition surveys, such as estimating young: adult-female ratio's, can be precluded by cost, safety, and feasibility. The use of remote cameras provides a potentially cutting-edge tool to apply to wildlife population estimation techniques. While the prevalence of remote cameras in ungulate studies has increased, few studies have used cameras to estimate vital rates, such as recruitment or survival. Here, we tested the potential of remote cameras to estimate calf: cow ratios and calf survival of elk (*Cervus elaphus*) using the Royle-Nichols (2003) occupancy model. Using the Royle-Nichols (2003) model, data collected from cameras on unmarked individuals can estimate detection probability and abundance.
We compared camera-based estimates of calf: cow ratio to traditional ground-based estimates obtained from group classification surveys. We test this approach in a partially migratory elk population at the Ya Ha Tinda (YHT) Ranch, Alberta, Canada. We deployed cameras (n=44), across the YHT, a working horse ranch and important elk winter range. We created a Royle-Nichols occupancy model for female and young-of-year elk, estimating abundance of respective age classes for a 110-day sampling interval between 15 May – 1 September 2018. We estimated calf survival by comparing the abundance estimates of calves between 7 primary sampling periods and determined the effect of abiotic, biotic and anthropogenic covariates on detection probability and abundance. Our camera-based ratio results made biological sense; following expected trends in detection variability, peak calf abundance, and declining ratios associated with neonatal mortality. We then compared the estimates of calf survival and group composition to those of traditional field estimates collected in the same time period. We conducted a Pearson correlation test and found an r=0.426 correlation between our camera-based and ground observations of calf:cow ratio. Although the correlation was moderate, ground-based estimates were biased due to sightability of hiding calves. Thus, our results demonstrate the utility of using remote cameras to derive important parameters for understanding ungulate population dynamics.

Acknowledgements

Funding for this project was provided by the American Indian College Fund, HOPA Mountain Native Science Fellows, Montana Institute on Ecosystems Alberta Environment, Parks Canada, Alberta Fish and Wildlife, Rocky Mountain Elk Foundation, Safari Club International – Foundation, Alberta Fish and Game Association, Alberta Conservation Association, Ministers Special License Funds, the Canadian National Sciences and Engineering Research Council (NSERC) Discovery grant to E.H. Merrill, and by the National Science Foundation (USA) Long-term Research in Environmental Biology grant (LTREB) to Mark Hebblewhite and Evelyn Merrill (1556248).

I thank Rick and Jean Smith, Parks Canada staff, for their generous hospitality and support of the research I conducted. I am forever grateful to Tom McKenzie and James Spidle for teaching me how to ride a horse and assisting me in servicing cameras. I thank the University of Alberta graduate students whom I learned so much from and developed lifelong friendships with; Jacky Normandeau, Kara MacAulay, Jodi Berg and Erik Spilker. I especially thank Mitch Flowers for his collaboration on this project, servicing far more cameras than I did and classifying hundreds of thousands of images. I thank Dr. Evelyn Merrill for her valuable insight, knowledge, and hospitality when I was in Edmonton. I also thank Dr. Robin Steenweg for helping me set-up cameras, understand how to properly log data, and classify images. I thank Dr. Mark Hebblewhite, my academic advisor, for his contagious enthusiasm, positivity, and encouragement. I thank Jesse Whittington for his tremendous support and willingness to share knowledge. I thank the Hebblewhite research lab for their acceptance of an undergraduate into the lab and their constant support for the research I conducted. I especially thank Hans Martin for his tremendous support in my undergraduate degree, you have made me a better field biologist,

leader, and instilled a wealth of statistical knowledge to me. I thank Lorina Keery for teaching me important plant ID skills and her constant support. I thank Dr. Josh Nowak for his friendship in the lab and the ice rink. I thank Dr. Mike Mitchell for his support on this project. I thank Craig Martynn for his friendship during my last year of undergraduate studies. Last, I wish to thank my parents and sisters for their support, especially my mom, Amy Conrad for her editing assistance. Because of the collaborate nature of this project I use the "we" voice throughout this undergraduate thesis.

INTRODUCTION

Understanding demographic vital rates is key to implementing effective management strategies, especially in harvested populations where harvest-success and population abundance is correlated to food-security, public support, and agency revenue (Sinclair et al. 2005; Mills 2013). Population biology is derived from vital rates such as birth-rates, juvenile and adult survival, density dependent factors, fecundity, immigration, and emigration (Pulliam et al. 1991; Sinclair et al. 2005; Bender 2006). Methods used to estimate such parameters are often limited in scope by agency resource availability, such as: cost, feasibility, safety, and personnel. Modern conservation requires novel methods in monitoring technique to maximize sound ecological inference while balancing fiscal and personnel constraints (Burton et al. 2015). Remote cameras are the nexus of ecological monitoring, and have pronounced potential to eventually replace invasive, unsafe, and costly methods of species monitoring (Moeller 2017).

Ungulate population dynamics are usually determined by the combination of constant, high survival in adult females, and highly variable survival rates in juveniles (Gaillard et al. 2000; Rathiel et al. 2007; Griffin et al. 2011). In large herbivores, adult female survival is commonly identified as the most important vital rate with the greatest influence on population growth rate (Nelson and Peek 1982; Escos et al. 1994; Walsh et al. 1995; Eberhardt 2002). However, understanding the factors that influence juvenile recruitment is equally important because ungulate population dynamics may be disproportionately affected by juvenile survival, given its variability and sensitivity to population density and environmental stochasticity (Coughenour and Singer 1996; Unsworth et al. 1999; Rathiel et al. 2007). Numerous studies across a range of taxa have suggested that juvenile survival is the predominant driver of ungulate

population dynamics (Chitwood et al. 2016). For example, studies of moose (*Alces alces*, Ballard et al. 1981), elk (*Cervus canadensis*, Rathiel et al. 2007), mule deer (*Odoicoileus hemionus*, Unsworth et al 1999), and roe deer (*Capreolus capreolus*, Gaillard et al. 1993) concluded that annual survival of juveniles varies dramatically compared to survival of prime aged adults. Thus, estimating juvenile survival is paramount to understanding the mechanics of population dynamics in ungulates (Gaillard et al. 2000) In addition, the degree of variance observed in both adult and juvenile survival is dependent on geographic occurrence of the species (Owen-Smith and Mason 2005). For example, elk populations inhabiting northern montane ecosystems are subject to more severe climatic pressures, density dependent effects, and multi-predator communities (Brodie et al. 2013). Comparatively, elk inhabiting the Eastern United States do not contend with such factors and employ higher survival rates than their Rocky Mountain counterparts (Brodie et al 2013; Fisichelli et al 2014). Conventual and emerging methods of monitoring elk, therefore, must have replicability across the diverse ecosystem's elk inhabit.

Traditional methods used to decipher demographic vital rates in ungulate studies include radio-telemetry (Unsworth et al. 1993; Raithel et al. 2007; Hebblewhite and Merrill 2011), and various indices including aerial counts (Storm et al. 2011), pellet counts, track surveys, and spotlighting (Fuller 1991; Collier et al. 2007). These indices, for example, aerial counts and spotlight surveys are plagued by issues of detectability bias, while pellet counts are challenged by variable defecation rates that cloud interpretation (Millspaugh et al. 2002; Duquette et al. 2014). Indices often lack scientific rigor and are becoming largely irrelevant in addressing ungulate population dynamic questions (Collier et al 2013). Agencies, therefore, often rely primarily on sightability adjusted aerial surveys or radio-telemetry studies to monitor population dynamics of ungulates (Harris et al. 2008). A suite of population and habitat inferences can be

determined by the use of radio-marking animals. Migratory behavior and influences of habitat can be studied using Global Positioning System (GPS) collars (Bishop et al 2005; Middleton et al. 2013). Cause-specific mortality in neonates can be examined by ear-tagging or use of expandable collars (Pojar et al. 2004; Raithel 2005; Berg 2019). Despite widespread acceptance and use, radio-collaring efforts present complex operational feasibility relating to cost, public relations (animal care), and safety. In addition, statistical assumptions must be met to estimate population vital rates from radio-telemetry including sufficient sample size, random sample and independence of monitoring sessions of marked animals (Duquette et al. 2014; DeCesare et al. 2016). These assumptions require large-scale efforts that are costly and resource intensive. This creates a niche for ecological monitoring to become cost-effective, non-invasive, and backed by statistical rigor that holds similar, if not more strength than traditional means of monitoring.

Recruitment is defined as the process in which new individuals enter a population (Sinclair et al. 2005). Specific to wildlife management of ungulates, this means recruitment of individuals that were born into the population and survived to a specific age-class, such as a reproductive adult (Schaub et al. 2006; Chandler et al. 2017). Traditional methods to estimate this critical parameter include aerial or ground surveys of group composition of young:adult ratios in late spring (Neal et al. 1983; Minta et al. 1989). These methods, however, especially aerial surveys are costly and unsafe. Capture-recapture methods are an alternative widespread framework for estimating recruitment with imperfect detection. There is a need for methods that can accurately identify trends in recruitment through space and time (Garton 2001; Hebblewhite and Merrill 2011).

Camera-trap surveys are emerging as a widely accepted metric population-level inference and have growing potential in the realm of ungulate studies (Royle and Nichols 2003; Fiske and

Chandler 2011). Uniquely identifiable species such as tigers (*Panthera tigris),* wolverines (*Gulo gulo*) and zebra (*Equus quagga*) allow camera-based studies to be used in spatially explicit capture-recapture models to estimate abundance (Royle et al. 2014). For most herbivores, individuals are not uniquely identifiable and therefore present researchers with a complex challenge of estimating demographic parameters in an unmarked population. However, there are a growing number of capture-recapture models designed to offer insights to abundance for unmarked animals such as ungulates (Royle and Nichols 2003; Chandler et al. 2013; Moller et al. 2018). *N*-mixture models are also used to estimate abundance of unmarked populations (Royle 2004) yet, they can be biased in populations where animals are detected at multiple cameras (Keever et al. 2017; Moeller 2017). Few studies have explored estimating juvenile recruitment in ungulates and the effectiveness of such methods compared to conventional studies**.** Chitwood et al. (2016) found that camera-based recruitment estimates were correlated to fawn (white-tailed deer, *Odocoileus virginianus*) survival estimates at Fort Bragg military instillation, North Carolina. Ikeda et al. (2013) conducted a similar study with Sika deer (*Cervus nippon*) in Japan and found camera and ground counts were correlated. Duquette et al. (2014) also found that inferences about white-tailed deer recruitment and population dynamics in the Upper Peninsula of Michigan were correlated from occupancy modeling and radio telemetry-based estimates. There are currently no studies on elk that compare remote-camera derived vital rates to conventional methods (ground observations, aerial counts etc.).

The objective of our study was to determine the potential for remote-cameras to provide reliable recruitment estimates in a well-studied elk population (Hebblewhite et al. 2006)**,** compared with more conventional methods of estimating recruitment such as ground-based surveys. Extensive long-term research has been conducted at the Ya Ha Tinda, Alberta,

examining factors that drive elk migration, adult survival, predation, calf survival from over 300 collared animals over 18 years (Hebblewhite and Merrill 2011; Hebblewhite et al. 2018). In addition, since 2013, there has been an extensive camera-trap sampling design overlaying the main winter range study area. This presents an ideal opportunity to test the relationship between conventional and modern techniques in monitoring elk recruitment. We hypothesized that our camera-based estimates would reflect similar trends in calf: cow ratios as our traditional ground-based monitoring methods.

METHODS

Study Area

The Ya Ha Tinda Ranch is a Parks Canada owned working horse ranch and is primary winter range habitat for the Ya Ha Tinda (YHT) elk population. The YHT is located on the east slopes of the Alberta Rocky Mountains, 13 km adjacent to Banff National Park (51'8'' 300 N, 115'8'' 300 W) and is approximately 4000 hectares and runs 17 km along the north bank of the Red Deer river under the jurisdiction of the Department of Canadian Heritage — Parks Canada Agency. Throughout the study area, topography varies from 1,600 meters to 2500 meters. The YHT is defined by rolling intact montane fescue (*Festuca campestris*) grassland surrounded by aspen (*Populus tremuloides*), Engelmann spruce (*Picea engelmannii*), and lodgepole pine (*Pinus contorta*) forests. Willows (*Salix spp.*) and dwarf birch (*Betula glandulosa*) are abundant in the grassland-forest ecotone. Average seasonal precipitation for 2018 was 398 mm (Government of Alberta 2018). From May to September during the study period, temperatures averaged 10˚C (ranging from -3˚C to 29 ˚C) and precipitation averaged 188 mm (Government of Alberta 2018)

Low precipitation and westerly winds (i.e., chinooks) keep the YHT relatively void of snow in the winter (Berg 2019). Ya Ha Tinda translates to "mountain prairie" in the Stoney-Sioux language, aptly describing the azonal, high-elevation, 20-km^2 montane rough fescue grasslands along the north side of the Red Deer River. The YHT represents one of the most pristine and largest rough fescue montane grasslands left in Alberta. Elk are the most abundant ungulate in the study area with a population that peaked in the 1990's at ~2000 individuals (Berg 2019). Elk demographic data collection began in 1985 (Morgantini and Hudson 1985) has been on-going since 2002 (Hebblewhite et al. 2006). Recent winter population-counts estimate the population to be stabilizing around ~400 individuals (Killen et al. 2016). The YHT elk population is partially migratory, with polymorphism for migrant and resident behavior. Migrant elk depart the winter range in May or June for summer ranges, returning to winter ranges from early September–November (Morgantini and Hudson 1989; Eggeman 2012; Berg et al. 2019).

Although elk dominated, white-tailed deer, moose, mule deer, and bighorn sheep (*Ovis canadensis*) persist in and around the ranch. Alternate prey species population trends are less well-known, whitetail deer have undergone significant population expansion in recent decades — bighorn sheep have been relatively stable while mule deer and moose appear to be declining. The YHT is home to a rich diversity of carnivores including grizzly bears (*Ursus arctos*), wolves (*Canis lupis),* black bears (*U. americanus*), cougars (*Puma concolor*), Canada lynx (*Lynx canadensis*) and coyotes (*Canis latrans*). Juvenile and adult elk primary sources of mortality are; wolves, grizzlies, cougars, and humans (during limited license hunt in the early fall and year-round First Nations' harvest).

Deployment

We deployed n=44 Reconyx (model HC600; HC900; Holmen, WI) in the winter of 2016/2017 in a previously established occupancy monitoring grid, *n*=7 (Steenweg et al. 2016) and an additional 37 cameras in an intensive 2.5 km^2 grid within the YHT ranch boundaries (Flowers 2019, Fig. 1). Camera locations were selected by a combination of systematic sampling (Steenweg 2016) and random placement within a systematic sampling grid (Flowers 2018). Cameras were deployed in accordance with Parks Canada Remote Camera Protocols (Heuer, Forshner, Whittington 2015) to maximize consistency for continued large scale camera-trap projects across study areas (Hunt and Bourdin 2015; Steenweg, Whittington, and Hebblewhite, 2015; Steenweg et al. 2016). Cameras were attached to trees at waist height. Settings were selected to "rapid-fire" to maximize photos of species, 5 photos were taken per trigger with no "time-out" between events. Vegetation was cleared in front of cameras to reduce false triggers from abiotic movement (wind-veg events). Cameras were serviced 2-3 times per-year to replace batteries, swap SD cards, and confirm alignment and function. Species were classified using Time-lapse software (Greenberg & Godin 2015) by trained technicians from the University of Montana and University of Alberta. YHT remote camera data was integrated into Parks Canada's Remote Camera database, contributing to multi-species monitoring efforts conducted across mountain parks.

We defined an event as a species (or group) that triggered photo sequences and were not separated from pictures by more than ten minutes. Elk events separated by more than 10 minutes were not considered a new event if there were other individuals present beyond the camera's field of detection throughout consecutive sequences. This can occur when the majority of a group has bedded down beyond the camera's range of detection and individuals closer to the

camera are photographed intermittently. This definition of an event was applied only when it could be confirmed that the same individuals are present in the background, recognized via unique collar IDs, antler configurations, or by remaining bedded in the same position throughout (Flowers 2019). Elk events were classified by denoting sex, age (young of year, yearling and adult), number of individuals, collar/tag visible, direction of travel, antler size, and any unique behavior. Photographs of human activity were subject to the same classifying protocol as wildlife and were denoted as either hikers or horseback riders (i.e. separate species for modelling purposes). Total counts of both humans and horses were recorded, it is important to note human pictures are deleted immediately after being integrated per Parks Canada protocol relating to privacy (Heuer, Forshner, Whittington 2015).

Study Period

We chose our sampling period based on the biological life history of calf elk in our study area. Our study period began 15 May 2018 and ended 1 September 2018, totaling 110 sampled days. The first calf to be detected by a camera was 15 May 2018. We ended our study period on September 1 for two reasons; first, elk calves begin to lose distinctive spots towards the end of August (Grant 1999; Beck et al. 2006), which could influence classifier error by mistaking large elk calves void of spots for yearling individuals. Second, a significant portion of migratory elk return to the YHT to breed in September (Hebblewhite et al. 2006, Eggeman et al. 2016). Thus, we ended our sampling period to prevent bias of age ratios due to the sudden influx of elk in our study area. The 110 days of camera-data was further partitioned into five, three-week sample intervals to best account for detection probability (i.e., hiding period) and calf phenology. Early-spring was defined between (15 May – 5 June), spring (6 June– 27 June), summer (28 June – 19 July), late summer (20 July – 10 August), and fall (11 August – 1 September). Ground

observation data was temporally partitioned identical to remote-camera data. We converted adult female and young of year data to detection/non-detection for each sample interval to model abundance.

Figure 1. Distribution of remote cameras (n = 44) across the winter range of the Ya Ha Tinda's partially migratory elk population in year 2018, along the eastern slopes of the Rocky Mountains adjacent to Banff National Park (green), Alberta, Canada.

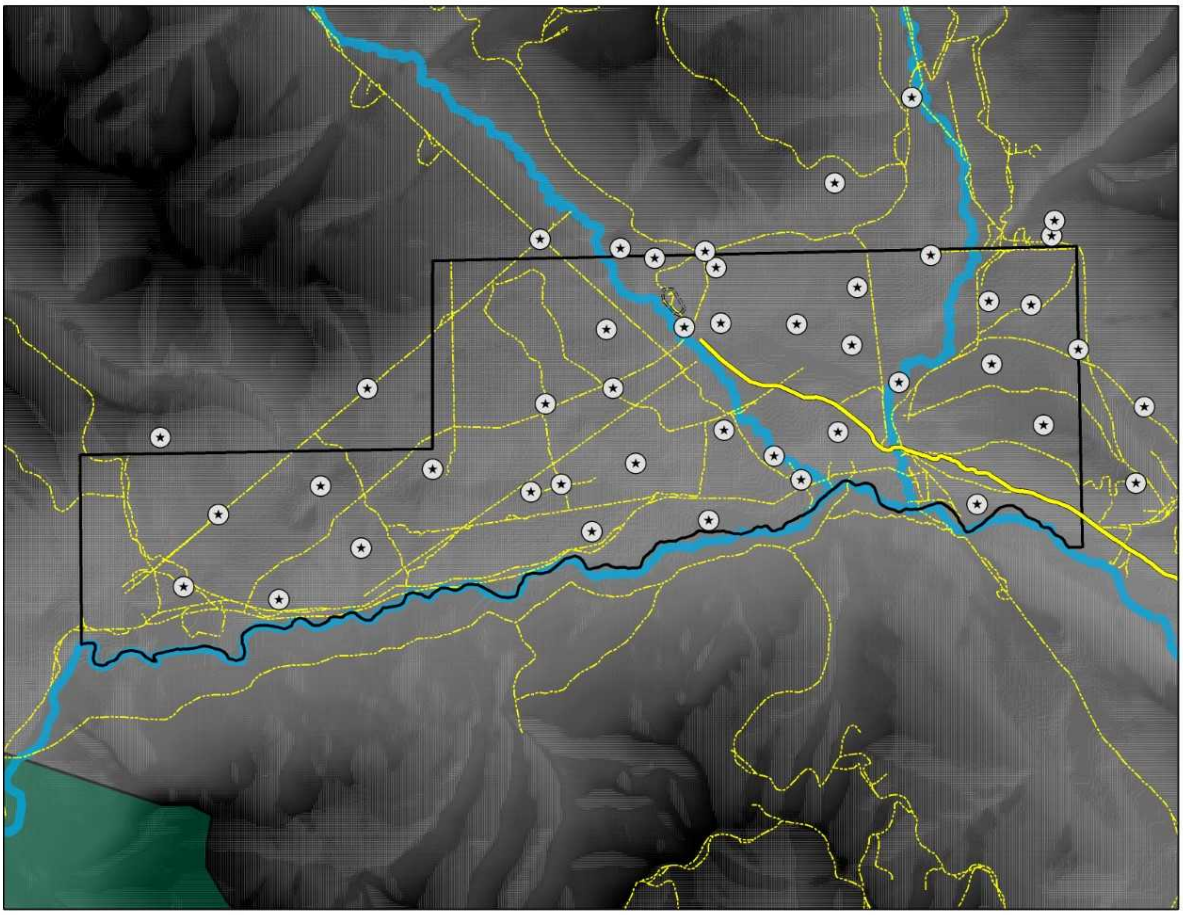

Statistical Modeling

We first fit the Royle-Nichols model to estimate adult and calf elk abundance using the occuRN function (see Royle and Nichols 2003, and below for details) in the package *unmarked* (Fiske and Chandler 2011) in program R (R Development Core 3.3 Team 2011). Next, we

describe this Royle-Nichols' (2003) model. We then estimate calf:cow ratios using standard ground based visual classification. Finally, we then compare estimated calf:cow ratios using our two methods (occuRN, ground) to test our hypothesis that remote camera-based estimates would be similar to conventional methods.

Royle-Nichols' Model

The occuRN function fits the latent abundance mixture model described in Royle and Nichols (2003), which uses binary detection/non-detection data of un-marked individuals by linking heterogeneity in detection probability to differences in site abundances modeled with a Poisson process (Royle and Nichols 2003). For detection to not occur at a site, none of the N_i animals present can be detected. If each animal has a probability r of detection, then overall detection probability of any individual is given by:

$$p = 1(1 - r)^k \qquad \text{(Eq. 1)}$$

where k is the number of sampling replicates and p is the sampling-replicate-specific detection probability (Royle and Nichols 2003; MacKenzie and Royle 2005). We defined k (sampling replicate) at 7 because detection probability estimates were closest to 0.80 when set to this number (M. Hessami, *unpublished data*). Data input for this model is based on binary, presence/absence outputs that are fitted to the occuRN function in program unmarked. The above equation operates under the transformation relating abundance to detection via the parameter r. Covariates of lambda (abundance) are modeled with the log link and covariates of r_{ij} are modeled with the logit link.

$$w_{ij} \sim Bernoulli(r_{ij}) \qquad \text{(Eq. 2)}$$

Thus, the detection (p) of a single individual in a sampled site (i) during a sample period (j) is modeled as a Bernoulli variable following:

$$p_{ij} = 1 - \left(1 - r_{ij}\right)^{N_i} \qquad \text{(Eq. 3)}$$

Where N_i is the local site abundance at site i. Next, the latent abundance, N_i, which is calculated the mean N per camera site is modeled as Poisson:

$$N_i \sim Poisson(\lambda_i) \qquad \text{(Eq. 4)}$$

Covariates

We adopted the classic recommended approach in fitting occupancy models by first determining covariates that affected detection probability, and second by then fitting covariates hypothesized to affect abundance in the occuRN model (Royle and Nichols 2003; Duquette et al. 2014). We considered both methodological and ecological covariates hypothesized to potentially affect both detection, *r*, and local abundance, N, at a camera site based on previous studies (Steenweg 2016, Steenweg et al. 2016). We used site and GIS-based landscape covariates to test their predictive power on detection and occupancy probabilities (Table 1). We centered and scaled each covariate to normalize differing metrics of performance within each site covariate. Within our tested covariates, we included four spatial increments of scale per covariate (500, 250, 100, 20 meter) to understand the degree of influence each biotic, abiotic, and anthropogenic covariate had on elk detection and occupancy. Further, we fit two sets of occuRN models following equation (1) for both elk calves (<4 months old) and adult female elk (> 1 year old). To further understand the effect of covariates on detection and following the occupancy modeling paradigm, we first modeled covariates hypothesized to affect *r*. Once we identified the best model for *r*, we proceeded to fit covariates on N.

Table 1. Camera site spatial and temporal covariates hypothesized to affect elk (*Cervus canadensis*) detection and abundance in Royle-Nichol's (2003) occupancy models using remote camera data (n=44) at the Ya Ha Tinda elk population range in Summer 2018.

Covariate	Acronym	Modeled on *r* (detection)	Modeled on *N* (abundance)
Biotic Variables			
Proportion of area burned (burns;at 3 scales)	burns	**X**	**X**
Normalized Difference Vegetation Index (NDVI; averages of July and August; 3 scales)	NDVI	**X**	**X**
-Dynamic Habitat Indices Seasonality (dhiseas; i.e. variability; 3 scales)	DHIseas	**X**	**X**
-Dynamic Habitat Indices cumulative (dhicum;i.e. total NDVI; 3 scales)	DHIcum	**X**	
-Dynamic Habitat Indices minimum (dhimin; 3 scales)	DHImin		**X**
-Land cover type(landcov), 7 levels:			
Open coniferous			
Closed coniferous			
Mixed deciduous			
Herbaceous			
Shrubs			
Abiotic covariates			
Topographic Position Index (TPI; at 3 scales)	TPI	**X**	
Anthropogenic covariates			
Distance to secondary road	d2road	**X**	**X**
Proportion of area cut (cuts; at 3 scales)	cuts	**X**	**X**
Regeneration forest (regen; cuts+burns; at 3 scales)	regen	**X**	
Distance to edge	d2edge	**X**	

Covariates were defined under three categories; biotic, abiotic, and anthropogenic. For Normalized Difference Vegetation Index (NDVI), we used maximum annual NDVI from year 2006. For human disturbance, we included distance to nearest secondary (or primary) road. To model terrain ruggedness, we created a topographical position index (TPI) using Land Facet Corridor Designer tools (Majka et al. 2007). TPI compares the terrain at a location to its surrounding area at a specific spatial scale where very negative values of TPI indicate low elevation compared to surrounding area (i.e. valleys) and positive values indicate higher elevations (i.e. peaks). Aspect, elevation and slope were estimated from a 30m resolution Digital Elevation Model. We then calculated slope using the Spatial Analyst extension for ArcGIS 9.3. For proportion of area burned, we calculated the proportion of the landscape that has burned in the last 115 years. We also included percent crown closure. We created a distance to streams covariate from a stream layer downloaded from www.GeoBase.ca. To categorize vegetation across the study area, we modified the landcover classification created by McDermid (2006) which used Landsat 5 Thematic Mapper (TM) and Landsat 7 TM sensors. We updated and consolidate this classification into 7 categories: open-coniferous, closed- coniferous, mixed-deciduous, herbaceous, shrubs, water, and rock-barren. All other raster covariates were also at 30m resolutions except NVDI (Steenweg 2016).

Model Selection

We conducted model selection on the detection process first for both calves and cow models, following advice from MacKenzie et al (2002). These models included detection set to constant (~1 ~1), covariates effecting detection (~1+ *covariate*) and a null model. We used the

package *corrplot* in program R 3.3 to screen for collinearity (r< 0.7) amongst covariates in fitted top-models. Second, we then ran another series of models based on top combined or single covariates on the abundance component, using the top detection models (MacKenzie et al. 2002). Remote-camera sites did not have bait, lure, and all cameras were the same make and model, thus we did not consider any such methodological covariates on *r*. Ultimately, we did not include any covariates on detection, and instead set detection as constant in our top unmarked models (see results). This was because there were trivial differences in *p* between top models with and without covariates (based on AIC), and because covariates did not make ecological sense (see Appendix A1 and discussion for details). We used a similar approach to conduct model selection for the best covariates affecting N, given the best detection model, as above. We conducted model selection for the top detection process using AIC_c the Akaike Information Criterion for small sample sizes (Steenweg 2016).

Deriving Abundance at a Site

Next, we estimated latent abundance at each site, *i,* using the ranef function in unmarked using the empirical Bayes method (Fiske and Chandler 2011). This function estimates the top occupancy model's posterior distributions for abundance (mean latent N for each site) at each site, and in each sampling period. This was then summed over all sites and used to derive the ratio of calves to females in each time period that we subsequently compared to ground observations. To derive a ratio, we then divided mean calf abundance by mean adult female abundance per sampling period (Duquette et al. 2016). We accounted for model selection uncertainty in our estimated abundance using model averaging approaches to obtain a model-averaged abundance estimate across top models using Akaike weights if there were multiple models within the top 0-2 Δ AIC_c (Burnham and Anderson 2002). Standard errors and

confidence intervals for camera-derived ratios were calculated using the bootstrapping method in program R (R Core development team 2018). We ran 10,000 iterations per sampling period to derive bootstrapped estimates.

Ground Observations

We conducted population classifications as frequently as possible throughout the study period whenever a group of elk was encountered. Observers approached a group of elk in an inconspicuous manner from the furthest distance possible. Observes then denoted group size, number of adult females, young of year, adult males, and yearlings following standardized protocols (e.g., Smith and McDonald 2002). We used the same sampling period (110 days) and five sampling intervals to estimate calf: cow ratios. Estimates were derived by dividing calf estimates by cow estimates for respective intervals. We estimated the variance using the cluster sampling method where we treated each ratio of elk as a cluster (Cochrane 1977: page 249, Samuel and Garton 1994; Hurley et al. 2011) where *R* is ratio of calves to adult females, f_i is the number of calves in a group. d_i represents the number of adult females per group, $\overline{d}$ is the mean number of adult females per group, *G* is the number of groups observed, and *N* the number of groups in the population (Equation 5)

$$\hat{V}\hat{R} = \frac{(1-\left(\frac{G}{N}\right))}{G\bar{d}^2} \frac{\sum_{i=1}^{G}(f_i-\hat{R}d_i)^2}{G-1} \quad \text{(Eq. 5)}$$

Correlation Between Ground and Camera Ratios

Lastly, we tested our hypothesis that remote-camera based calf:cow ratios would be closely correlated with ground-based estimates. We estimated the correlation coefficient between our camera- and ground-obtained estimates of calf:cow ratio using Pearson's correlation coefficient. Second, we conducted linear regression to estimate the intercept (β_0) and regression coefficient (β_1) for the relationship between remote-camera ratios and ground observation ratios.

If ground and camera observations are perfectly correlated, then the β_1 coefficient should be not significantly different than one (Ikeda et al. 2013; Chitwood et al. 2017). Similarly, if $\beta_0 = 0$, then both estimators could be interpreted as being unbiased, at least with respect to each other.

RESULTS

Of the 44 camera's we deployed, we used data from 37 operational cameras from the spring and summer of 2018 that we used in subsequent analyses.

Detection

Overall, there were a variety of spatial covariates that seemed potentially important in affecting detection, *r*, with a constant N model (Appendix Table A1). For example, our top model for detection of calves in time period 1 was distance to road (ndist_road.s) with a back-transformed logit *r* value of 0.0248 (SE= 1.062, Appendix Table A1). In the subsequent 4 time periods, *r* was affected by Dynamic Habitat Indices, and distance to edge (SE= 0.232, 0.036, Appendix Table A1). Adult Female top detection models had similar results with distance to road also showing the greatest effect on detection in time period 1, with a r value of 0.024 (SE= 0.064, Appendix Table A2). In most top model sets, i.e., 0-4 ΔAIC, there was also the null model (~1 ~1) indicating support for constant detection for calf elk. Because the best model in the presence of covariate effects on N usually resulted in the null model for detection (see below, Appendices), we proceeded using the constant only detection for subsequent models.

occuRN Models

Calves

Overall, calf elk abundance models were driven by habitat productivity variables such as the Dynamic Habitat Index (DHI), NDVI, or regenerating vegetation at various scales (Table 4)

). Most interestingly, however, for all of our final calf abundance models, the top model for detection was the constant model when evaluated in the presence of the spatial covariates on abundance (Appendix Table A1). We discuss the evident substitution of covariate effects between p and N in the discussion but proceed reporting our top occuRN models with constant p for elk calves. As a reminder, all covariates are reported in the standard deviation scale, and we only report coefficient estimates for the top model for brevity.

In the early spring, the top model for elk calves showed abundance increased with greater regeneration landcover classes within 500 m ($\beta_1 = 0.057$, SE = 0.363, Table 4). In the spring, abundance increased with Dynamic Habitat Index scores within 100m ($\beta_1 = 0.014$, SE = 0.623). For our third sampling period, summer, calf abundance increased with a decreased distance from roads ($\beta_1 = 0.070$, SE = 0.983). For our fourth sampling period, late summer, abundance increased with higher NDVI August scores ($\beta_1 = 0.047$, SE = 0.974), decreased distance to roads ($\beta_1 = 0.055$, SE = 0.881), and Dynamic Habitat Index score at the 100 meters scale ($\beta_1 = 0.137$ SE = 0.519). For our last time period, fall, Dynamic Habitat Index score within 100m increased abundance ($\beta_1 = 0.280$, SE = 1.50).

Adults

Overall, adult female abundance models were driven by habitat productivity variables such as the dynamic habitat index, NDVI, or regenerating vegetation at various scales (Table 5). Similar to calves, however, the top model for detection of adults was also the constant model when evaluated in the presence of the spatial covariates on abundance (Appendix Table A2). In the early spring, adult female abundance increased with decreasing distance from road, increased with NDVI score at the 20m scale ($\beta_1 = 0.074$, SE = 0.911), and increased with DHI at the 100-meter scale ($\beta_1 = 0.047$, SE = 0.974). In the spring time period, abundance also increased with

Dynamic Habitat Index scores within 100m (β_1 = 0.039, SE =0.980). For our third sampling period, summer, adult female abundance increased NDVI scores at the 20m scale (β_1 = 0.744, SE = 0710). For our fourth sampling period, late summer, abundance increased greater distance from roads (β_1 = 0.023, SE = 0.214), Dynamic Habitat Index scores within 100 meters (β_1 = 0.057, SE = 0.233), and NDVI scores at the 20m scale (β_1 = 0.086, SE =0.580). For our last time period, fall, regeneration within 500m increased adult female abundance (β_1 = 0.021, SE = 0.603).

Abundance Estimates

Calf Abundance

We recorded 989 elk events in our sampling period with 449 calf elk events. Most calf events were with a female, but there were 59 events of only a calf detected on a camera. Because of model selection uncertainty (Table 4, we report model averaged abundance estimates. Total model-averaged abundance for *early spring* calf estimate was: 26.27 (SE: 0.443), *spring* 174.60 (1.473), *summer* 26.80 (0.514), *late-summer* 20.57 (0.529), *fall* 65.70 (0.806, Table 3).

Adult Female Abundance

We recorded 930 adult female elk events from a total of 989 elk events. Because of model selection uncertainty (Table 5) we report model averaged abundance estimates. Total model-averaged abundance for *early spring* adult female estimates were:116.85 (SE: 1.442), *spring* 225.70 (1.844), *summer* 86.04 (0.949), *late-summer* 71.86 (1.014), *fall* 338.98 (2.190, Table 2).

Remote Camera Calf:Cow Ratios

The corresponding *early spring* calf: cow ratios were: 0.230 (95% CI, 0.05 — 0.633, Figure 2), *spring* 0.77 (0.021 — 0.576), *summer* 0.31 (0.467 — 0.761), *late-summer* 0.29 (0.067 — 0.553), *fall* 0.19 (0.07 — 0.741, Figure 2).

Correlation between Camera-based and Ground Ratios

We conducted 136 population classifications of the YHT elk population between 15 May – 1 September 2018. The *early spring* calf:cow ratio was: 0.040 (SE: 0.006), *spring* 0.138 (0.011), *summer* 0.250 (0.013), *late-summer 0*.321 (0.025), *fall* 0.257 (0.02187, Table 6). These results had moderate correlation with the camera-based estimates (Figure 3), except during the spring period when ground estimates were 0.637 lower than estimates from the remote cameras. Considering all 5 time periods, the correlation between ground and camera estimates was only r = -0.223, p = 0.711, n=5. Moreover, the linear regression estimate of $\beta_0 = 0.46$ (SE =0.2652), and $\beta_1 = -0.51$ (SE= 1.181), indicating no significant relationship between ground and camera estimates.

However, if we remove the spring period when estimates were divergent, the correlation coefficient improved dramatically to r = 0.426 (p = 0.57, n=4). Moreover, the $\beta_0 = 0.21$ (SE = 0.068) indicating minimal bias, and $\beta_1 = 0.19$ (SE=0.286), indicating a moderate correlation between the two methods.

Table 2: Remote-camera estimates of adult female elk abundance from each 5-week sampling interval. Models were ranked using Akaike's Information Criterion and *K* is the number of parameters. Estimated adult female site and detection probabilities and standard deviation (SD) of site abundance (summation of mean N abundance per site) or detection (logit-scale) are presented.

Time Interval	***r, p****	**Top Abundance Model**	**K**	**N(Abundance)**	**SD**
Early Spring 15 May-5 Jun	0.0159; 0.99	~1 ~ 1 + NDVIAug20.s + ndist_road.s + dhimin100.s	5	116.85	0.949
Spring 6 Jun – 27 Jun	0.0473; 0.99	~1 ~ 1 + dhiseas100.s	3	225.70	1.844
Summer 28 Jun – 19 Jul	0.0744;0.99	~1 ~ 1 + NDVIJul20.s	3	86.05	0.949
Late Summer 20 Jul – 10 Aug	0.0855;0.99	~1 ~ 1 + NDVIAug20.s + ndist_road. s + dhimin100.s	4	71.86	1.014
Fall 11 Aug – 1 Sept	0.0212;0.99	~1 ~ 1 + regen500.s	3	338.98	2.190

Table 3: Remote-camera estimates of calf elk (< 4 months old) elk abundance from each 5-week sampling interval. Models were ranked using Akaike's Information Criterion and *K* is the number of parameters. Estimated adult female site and detection probabilities and standard deviation (SD) of site abundance (summation of mean N abundance per site) or detection (logit-scale) are presented.

Time Interval	*r, p*	Top Abundance Model	K	N(Abundance)	SD
Early Spring ***15 May-5 Jun***	0.057;1	~1 ~ 1 + regen500.s	3	26.27	0.443
Spring ***6 Jun – 27 Jun***	0.013;1	~1 ~ 1 + dhiseas100.s	3	174.60	1.473
Summer ***28 Jun – 19 Jul***	0.070;1	~1 ~ 1 + ndist_road. s	3	26.79	0.514
Late Summer ***20 Jul – 10 Aug***	0.137; 0.99	~1 ~ 1 + NDVIAug20.s + ndist_road. s + dhimin100.s	5	20.57	0.529
Fall ***11 Aug – 1 Sept***	0.029;1	~1 ~ 1 + dhiseas100.s	3	65.69	0.806

Table 4. Top (≤ 2 ΔAIC) occuRN abundance models for calf elk for the 5 sampling period 2018, Ya Ha Tinda ranch, Alberta, Canada. For each time period, model structure of the occuRN model is given as first the covariates affecting detection, ~1, and second, the covariates affecting the latent abundance, ~ 1 + . See Table 1 for covariate names. Models are reported in rank order by ΔAIC, with reported Akaike weights, latent abundance (N) for each model, and then the model averaged weighted N for that time period.

Time	**Model**	**ΔAIC**	**AIC weights**	**N**	**Weighted N**
Early Spring	~1 ~ 1 + regen500.s	0	0.258	23.56	26.27
	~1 ~ 1 + burns500.s	1.60	0.116	22.26	
	~1 ~ 1 + dhiseas100.s + regen500.s	1.82	0.103	23.97	
	~1 ~ 1 + ndist_road.s	1.87	0.101	23.34	
Spring	~1 ~ 1 + dhiseas100.s	0	0.309	163.42	174.60
	~1 ~ 1 + burns500.s + dhiseas100.s	1.77	0.141	165.13	
	~1 ~ 1 + dhiseas100.s + regen500.s	1.72	0.131	167.48	
	~1 ~ 1 + dhicum100.s	1.95	0.117	185.50	
Summer	~1 ~ 1 + ndist_road.s	0	0.136	29.90	26.80
	~1 ~ 1 + dhimin100.s	0.79	0.091	23.33	
	~1 ~ 1 + regen500.s	0.96	0.083	25.56	
	~1 ~ 1 + dhiseas100.s	0.97	0.083	22.32	
	~1 ~ 1 + burns500.s + dhiseas100.s	0.97	0.083	27.02	
	~1 ~ 1 + dhiseas100.s + regen500.s	0.99	0.082	29.95	
	~1 ~ 1 + burns500.s	1.67	0.079	22.77	
	~1 ~ 1 + NDVIJul20.s	1.69	0.058	21.77	
Late Summer	~1 ~ 1 + NDVIAug20.s + ndist_road.s + dhimin100.s	0	0.249	24.24	20.57
	~1 ~ 1 + dhicum100.s + ndist_road.s +	1.45	0.120	22.73	
Fall	burns500.s				

~1 ~ 1 + ndist_road.s + dhicum100.s + burns500.s	1.45	0.120	22.73	
~1 ~ 1 + NDVIJul20.s + dhimin100.s + regen500.s + burns500.s	1.65	0.109	19.70	
~1 ~ 1 + dhiseas100.s				
~1 ~ 1 + dhimin100.s	0	0.139	72.24	65.69
~1 ~ 1 + dhicum100.s	0.39	0.114	64.50	
~1 ~ 1 + burns500.s	0.51	0.108	64.67	
~1 ~ 1 + NDVIJul20.s	1.01	0.084	62.62	
~1 ~ 1 + ndist_road.s	1.03	0.083	61.68	
~1 ~ 1 + dhiseas100.s + regen500.s	1.12	0.079	62.40	
	1.97	0.084	74.02	

Table 5. Top (≤ 2 ΔAIC) occuRN abundance models for Adult Female elk for the summer sampling period 2018, Ya Ha Tinda ranch, Alberta, Canada. For each time period, model structure of the occuRN model is given as first the covariates affecting detection, ~1, and second, the covariates affecting the latent abundance, ~ 1 + . See Table 1 for covariate names. Models are reported in rank order by ΔAIC, with reported Akaike weights, latent abundance (N) for each model, and then the model averaged weighted N for that time period.

Time	**Model**	**ΔAIC**	**AIC weights**	**N**	**Weighted N**
Early Spring	~1 ~ 1 + NDVIAug20.s + ndist_road.s + dhimin100.s s	0	0.558	140.76	116.85
	~1 ~ 1 + dhiseas100.s	0	0.290	231.36	225.70
Spring	~1 ~ 1 + burns500.s + dhiseas100.s	1.79	0.119	230.48	
	~1 ~ 1 + dhiseas100.s + regen500.s	1.98	0.107	232.94	
Summer	~1 ~ 1 + NDVIJul20.s	0	0.239	78.13	86.05
	~1 ~ 1 + NDVIAug20.s	0.56	0.180	76.44	
Late Summer	~1 ~ 1 + NDVIAug20.s + ndist_road.s + dhimin100.s	0	0.150	86.53	71.86
	~1 ~ 1 + dhicum100.s + ndist_road.s + burns500.s	0.48	0.118	85.44	
	~1 ~ 1 + ndist_road.s	0.79	0.103	65.31	
	~1 ~ 1 + regen500.s	1.46	0.073	62.99	

Fall	~1 ~ 1 + regen500.s	0	0.251	318.91	338.98
	~1 ~ 1 + ndist_road.s	1.65	0.109	362.46	
	~1 ~ 1 + dhiseas100.s + regen500.s	1.91	0.096	317.92	

Table 6: Ground estimates of Ya Ha Tinda, Alberta, elk population calf:cow ratios from each 5-week sampling interval. Estimates were derived by summing total calf and total adult female group counts and dividing values to derive a ratio. Variance was calculated using the cluster sampling method (Cochrane 1977: page 249, Samuel and Garton 1994; Hurley et al. 2011).

Time Interval	**calf:cow ratio**	**95% confidence Intervals**
Early Spring; 15 May-5 Jun	0.04	0.027—0.053
Spring; 6 Jun – 27 Jun	0.137	0.115—0.159
Summer; 28 Jun – 19 Jul	0.25	0.222—0.278
Late Summer; 20 Jul – 10 Aug	0.32	0.270—0.370
Fall; 11 Aug – 1 Sept	0.25	0.206—0.294

Figure 2. Sampling intervals on the X axis (three week-intervals) and calf:cow ratio value on the Y axis from derived remote camera (green) and ground estimates (orange) of the Ya Ha Tinda, Alberta, Canada elk population. 95% confidence intervals are shown on error bars.

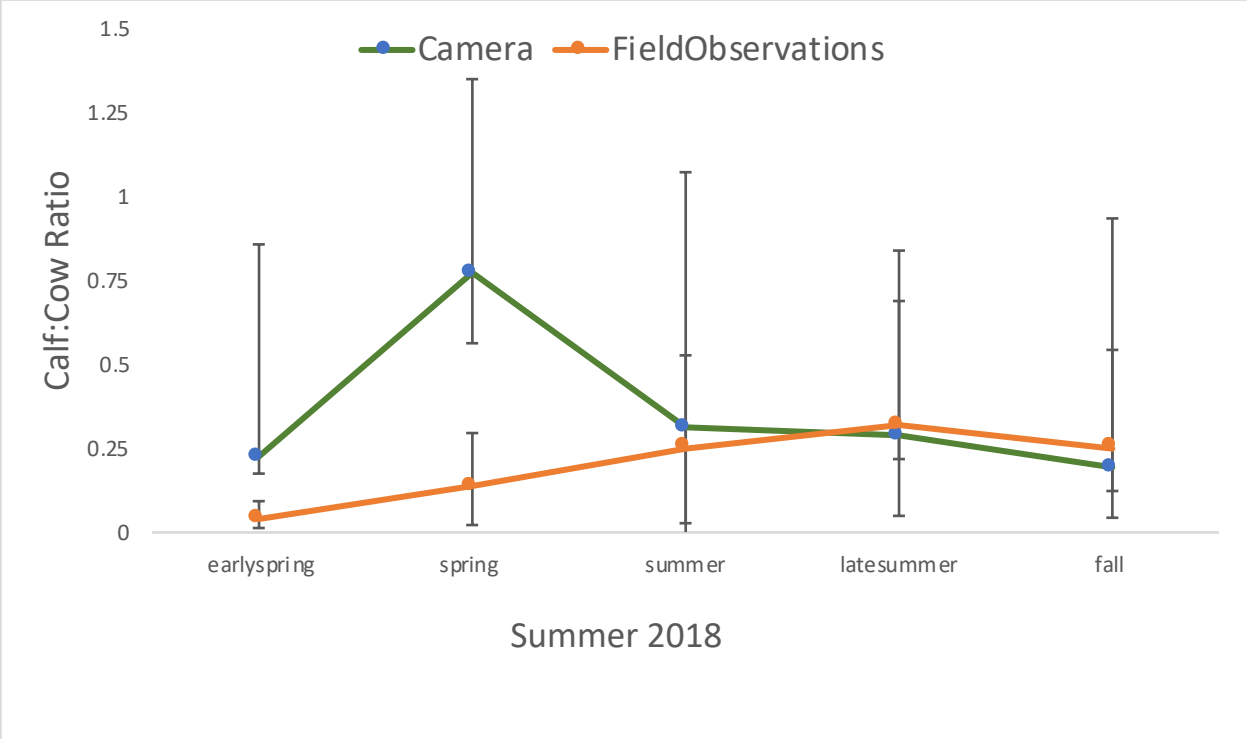

Figure 3. Relationship between ground (X) and camera-based calf:cow (Y) ratio's at the Ya Ha Tinda ranch, Alberta, 2018 showing a) the correlation for all 5 time periods (R^2= -0.240, y= 0.460x – 0.51), and b) same but with just 4 time periods, excluding the outlier, spring (R^2=0.426, y=0.213x + 0.19).

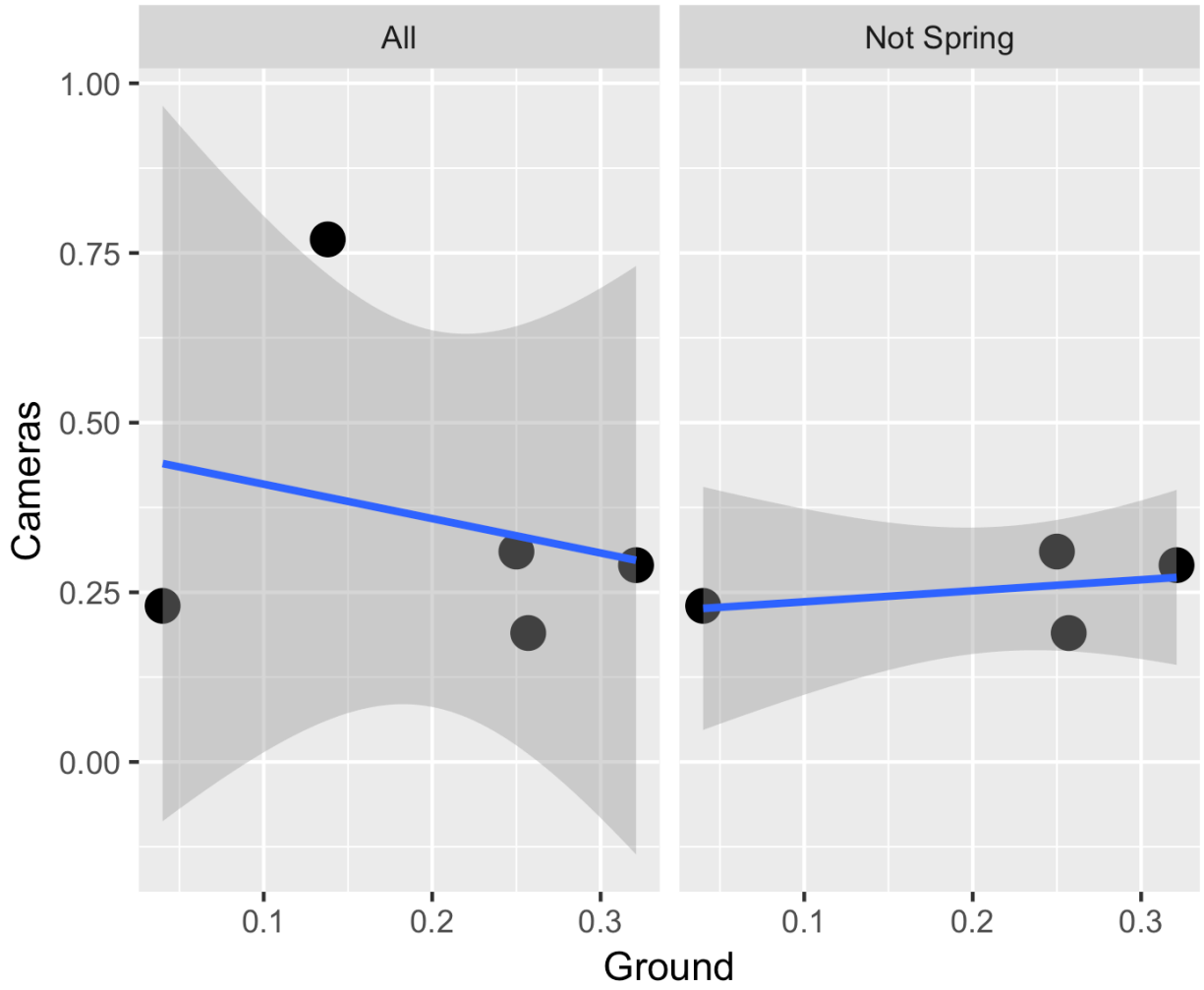

DISCUSSION

Our results offer the first empirical comparison of juvenile elk recruitment ratios derived using two methods; remote cameras and traditional ground observations. Ground observation and Royle-Nichols (2003) occupancy models corroborated initial differing trends in calf:cow ratios over the summer of 2018. Remote-camera ratio estimates made more biological sense when compared to ground observations in terms of timing of low, peak, and declining abundance. Many field studies of neonatal elk calf survival support our remote-camera trend in calf elk survival (Rathiel 2007; Griffin et al. 2011; Berg 2019). Namely, like many other ungulates, elk calf abundance peaks in early spring soon after birth, but rapidly declines following high neonatal (first 4-6 weeks) mortality (Berg 2019). Ground observations roughly corresponded to our remote-camera based estimates, with the exception of the second spring time period. However, this time period immediately follows birth, and is associated with sightability bias of the hiding behavior of neonate elk calves during this time period (Johnson 1951). Thus, consideration of the biology of elk calves, and comparison to studies of marked elk calves further supports our hypothesis that remote cameras can estimate juvenile recruitment rates of elk and potentially replace traditional costly, labor intensive methods.

Low sightability of elk (and other ungulates) during the 'hiding' phase lead to what we believe were biologically unrealistically low ground-based estimates in our second time period (0.138 vs 0.77). Thus, it seems remote cameras can effectively detect and estimate local calf abundance during the hiding phase compared to ground based estimates. For the spring time period, calf:cow ratios was (0.770), reflecting the highest abundance of elk calves in keeping with previous studies in our study area of neonatal elk calf survival and abundance (Berg 2019).

In fact, this estimate, 0.77, makes biological sense given the high pregnancy rates of adult (> 2-year-old) females in our population (Hebblewhite and Merrill 2011), and lower yearling pregnancy rates. This peak in recruitment ratio is likely a biologically realistic depiction of the rapid change in both the abundance and behavior of neonate calves as they transition from the hiding calf rearing phase, to the nursery and group integration phase (~26 days old) joining the population, increasing mobility, and thus detection (Grant 1999; Berg 2019). Thus, when examining the correlation between ground and remote-camera based estimates, we removed this outlier (spring) from both camera-based estimates and ground estimates when we conducted our Pearson's correlation to better model the relationship of recruitment (r=0.426, Figure 3b). Although our correlation is moderate between sampling methods, we believe our camera-based estimates depicted a more precise estimate of calf recruitment compared to ground observations and show promise as a method to non-invasively estimate ungulate recruitment.

While our study provides the first evidence that remote cameras may provide a useful method for elk population monitoring, our results echo previous studies in other systems and species. For example, Chitwood et al. (2017) used known-fate modeling in program MARK to compare fawn survival rates based on radio-collar data to estimates of recruitment derived from camera-trapping efforts. They further assessed the relationship between survival and recruitment by using a Pearson's correlation. Their results showed a strong correlation (R^2 value 0.758) between camera-based recruitment and radio collar-based survival when assessing year to year trends. In relation to our study, Chitwood et al. (2017) study design is similar to ours in the comparisons they conducted, yet they report a longer sample duration (6 years) and in turn produce more robust results assessing the relationship between their tested methods. Future studies could compare previously collected neonate elk calf survival in our study area (Berg

2019) to remote camera estimates. Ikeda et al. (2013) evaluated the use of camera-trapping for estimating population composition of sika deer in Japan. However, like our study, they did not have marked neonate elk calves, but compared cameras to ground estimates. Their results cast doubt on the biological realism of their camera data to track fawn:doe ratio, seemingly because of the challenge of low detection of fawns during the birth pulse. However, their doe:buck ratios showed seasonal patterns that made biological sense.

Finally, Duquette et al. (2014) employed the most similar study to ours by comparing radio-telemetry and occupancy modeling using the Royle Nichols (2003) model to estimate population growth (λ) in white-tailed deer. They found estimates derived by radio-telemetry provides more precise population growth estimates whereas camera-based estimates had wide confidence intervals. Unmarked adult female abundance and fawn: doe ratios generally reflected trends in radiomarked deer survival and recruitment (Duquette et al. 2014). Review of these studies suggest that under certain conditions, remote cameras may be an effective means of tracking recruitment of ungulates in the neonatal period.

We found no covariates with consistent effects on detection, especially when combined with the abundance part of the occuRN model. Our study design used no known methodological factors such as baits, lures, or differences in camera types that may have affected the detection process (Steenweg 2016; Chitwood et al. 2017). While a previous large carnivore occupancy study conducted by Steenweg et al. (2016) at the YHT concluded camera-type (flash, no flash) bait and lure (selective sampling) were covariates that influenced the detection probability per camera site. Our study had no scent attractants or bait, and camera models stayed consistent throughout (Reconyx Hyperfire HC600 & HC900). In our first phase of model fitting, our top covariates affecting detection (when abundance was modeled as a constant, ~ 1) were DHI,

NDVI, and distance to road (see appendix A1). However, especially when combined with the top ecological covariates, it seemed that these ecological covariates had stronger effects on the abundance process, and the top detection models were almost always simply constant detection models. This interpretation is bolstered by the similar covariate coefficients when included in the p and N parts of the occuRN models. There may be some unknown substitution between detection and ecological covariates in occuRN models that warrant further exploration. Regardless, in conclusion, we kept detection constant and did not include top covariate affecting models on abundance (N) estimates.

Like any model, the Royle-Nichols (2003) model assumes that: 1) occupancy state at a site remains constant throughout the season (population closure in the case of the occuRN model). there is population closure within a sampling period, 2) detection events are independent, and 3) detection probability of a single animal is assumed to be constant across time. When applying a model to a new scenario, such as estimating calf:cow ratios, it is important to assess assumptions (Duquette et al. 2014). First, because of high adult female elk survival, the assumption of closure seems reasonable for adults (e.g., summer survival is > 0.92, Hebblewhite et al. 2018). However, this assumption is more problematic for calves, obviously, because of the strong neonatal mortality hazard (Griffin et al. 2011; Berg 2019). Yet, we feel that within our 5-week time periods, the assumption of closure for elk calves is approximate. More broadly, we limited our sampling period to summer (September 1) to avoid problems with population closure triggered by the return migration of the migratory component of the population (Hebblewhite et al. 2006). Future studies could develop separate winter seasonal models to estimate calf:cow ratio's during winter. The main second assumption is the assumption of independence in detection, especially given elk are classically a group-living

species. While we did not extend the Royle-Nichols's model to account for group-level detection, it could be possible to model the abundance of elk groups, augmented with additional information about average elk group size to estimate elk abundance. Regardless of these challenges with the assumptions of our model, the close correspondence between our abundance estimates from the occuRN models and field counts (see below) reassures our interpretation of our results as providing biologically interpretable results.

The reported abundance estimates derived from the ranef function in the R package unmarked produced believable abundance estimates for adult female and calf elk. Indeed, some abundance estimates appear to be skewed in relation to the actual abundance of elk on the landscape at the sampled period (Table 2 and 3). We strengthened our reported abundance estimates by conducting Akaike weights (Burnham and Anderson 2002) to account for model selection uncertainty across our top occuRN models from our 17 top models for each time period. For example, in the second sampling period (*spring)*, both calf and adult female elk reported abundance estimates of 163.4 and 231.4 individuals respectively. These modeled averaged abundance estimates roughly correspond to maximum ground counts of adults and calves obtained in the summer of 182 total individuals (M. Hessami, unpublished data). The processes influencing this high estimate could be: a) migration and parturition plasticity– in which adult females return to the resident herd after rearing calves to adequate mobility (~3 weeks old); or b) group size of elk is not being explicitly accounted for in the occuRN model. Important to the scope of this paper, the attributed calf:cow ratio with this time period does make biological sense and therefore supports the precision of the occuRN model in estimating recruitment rates in the YHT elk population. Thus, we feel justified in our interpretation and

cumulative impact our study has on the ability to model juvenile recruitment in a partially migratory elk population.

The correlation between remote camera and ground-based estimates was not perfect, suggesting one method may be better at tracking trends in calf survival over a summer interval. But without a known reference sample, such as radiocollared animals, interpretation of which method is 'best' is challenging. Similar to Ikeda et al. (2013), our two early sampling periods (early spring, spring) could be biased by low detection associated with calves in hiding. There have been two studies that have compared radiomarked or individually recognizable individual survival rates to recruitment rates from cameras. The first we discussed in the introduction, by Chitwood et al. (2017) that showed close correspondence between visual observations and fawn survival rates over 6 years in 2 study areas. Second, Chandler et al. (2017) used individually recognizable spot patterns on key deer neonatal fawns to track survival using a Spatially-Explicit-Capture-Recapture framework. He also showed close correspondence between this independent estimate of the neonate survival rate and biological expectations from other neonatal studies. However, unlike these two studies, we did not have a metric of truth to compare our results with because obtaining a census in this population, like most other wildlife studies, this would be extremely difficult, if not possible. Future studies with these data may be able to compare remote camera-based estimates of recruitment with neonatal elk calf survival from Berg (2019)'s marked elk calves in 2017. Uncertainty in truth is prevalent in most ungulate studies, unless the population is closed (fenced), or marked or individually recognizable individuals offer an approach to estimate survival rates (Fiske and Chandler 2011; Erbert et al. 2012; Zero et al. 2013). Regardless of these difficulties, our study revealed that ground estimates have unreliable recruitment estimates for calf elk due to sightability bias in the early calf-rearing stage.

Our research was motivated by the need to develop more precise, non-invasive and large-scale sampling techniques to better monitor a critical parameter of elk life history. The Ya Ha Tinda elk herd is a cultural keystone species, providing food security for the Stoney Sioux First Nations (Johnson 2012), trophy bull opportunity via a coveted limited entry draw system (Government of Alberta 2017), and recreational opportunity for the general public. Thus, reliable annual estimates of population vital rates are paramount for sound management decisions. Current research at the YHT seeks to develop integrated population models (Abadi et al. 2010) that capture dynamic and complex annual ecological process and produce precise population estimates for management purposes. Our study provides reliable camera-based recruitment estimates that will be incorporated in integrated population models in the future. Moving forward, it could be profitable to compare our results to Berg (2019) calf survival study conducted at the YHT between 2013-2016, similar to Chitwood et al. (2017). Furthermore, this approach could also be used to estimate bull:cow ratios similar to Ikeda et al. (2013) for Sika deer in Japan, but with comparison to radiocollar-informed estimates of bull:cow ratios.

The use of remote-camera surveys in population monitoring is becoming more common. Advances in camera technology, reduction in cost, and scientific studies demonstrating their power are promulgating their acceptance in wildlife management. Large networks of remote cameras could lead to robust monitoring networks capable of detecting changes in animal distribution and abundance (Steenweg et al. 2017). Automated classification programs are easing the ability of such camera networks to generate useable data (Tabak et al. 2019). Our methods have replicability potential to more species than just elk, including other ungulates whom neonates are followers from birth (moose, caribou; *Rangifer tarandus)* instead of hiders (elk, mule deer, antelope). Western Provinces and States are often limited in ability to adequately

monitor game-species due to expansive management areas and cost (Timmerman 1993). Aerial surveys are expensive and risky yet are a predominate method of estimating population vital rates in harvested species across the Western US and Canada (Gasaway et al. 1986; Caughley and Sinclair 1994; Moeller 2017). The application of remote cameras could help improve data-collection practices and contribute to needed advances in wildlife management.

LITERATURE CITED

Abadi, F., Gimenez, O., Arlettaz, R., & Schaub, M. 2010. An assessment of integrated population models:bias, accuracy, and violation of the assumption of independence. *Ecology*, **91**, 7-14.

Ballard, W. B., Spraker, T. H., & Taylor, K. P. 1981. Causes of neonatal moose calf mortality in south central Alaska. *The Journal of Wildlife Management*, **45**, 335-342.

Beck, J. L., Peek, J. M., & Strand, E. K. 2006. Estimates of elk summer range nutritional carrying capacity constrained by probabilities of habitat selection. *The Journal of Wildlife Management*, **70**, 283-294.

Bender, L. C. 2006. Uses of herd composition and age ratios in ungulate management. *Wildlife Society Bulletin*, **34**, 1225-1230.

Berg, J. 2019. Shifting strategies: Elk calf survival in a partially migratory elk herd. Doctoral Dissertation. Department of Biological Sciences. University of Alberta, Edmonton, Alberta.

Bishop, C. J., Unsworth, J. W., & Garton, E. O. 2005. Mule deer survival among adjacent populations in southwest Idaho. *The Journal of Wildlife Management*, **69**, 311-321.

Brodie, J., Johnson, H., Mitchell, M., Zager, P., Proffitt, K., Hebblewhite, M., ... & Gude, J. 2013. Relative influence of human harvest, carnivores, and weather on adult female elk survival across western North America. *Journal of Applied Ecology*, **50**, 295-305.

Burton, A. C., Neilson, E., Moreira, D., Ladle, A., Steenweg, R., Fisher, J. T., ... & Boutin, S. 2015. Wildlife camera trapping: a review and recommendations for linking surveys to ecological processes. *Journal of Applied Ecology*, **52**, 675-685.

Chandler, R.B. & Royle, J.A. 2013. Spatially explicit models for inference about density in unmarked or partially marked populations. *The Annals of Applied Statistics,* **7,** 936-954.

Chitwood, M.C., Lashley, M. A., Kilgo, J. C., Cherry, M. J., Conner, L. M., Vukovich, M., ... & Moorman, C. E. 2017. Are camera surveys useful for assessing recruitment in white-tailed deer? *Wildlife Biology*, **17**, 33-37.

Collier, B. A., Ditchkoff, S. S., Raglin, J. B., & Smith, J. M. 2007. Detection probability and sources of variation in white-tailed deer spotlight surveys. *The Journal of Wildlife Management*, **71**, 277-281.

Collier, B. A., Ditchkoff, S. S., Ruth, C. R., & Raglin, J. B. 2013. Spotlight surveys for white-tailed deer: Monitoring panacea or exercise in futility? *The Journal of Wildlife Management*, **77**, 165-171.

Coughenour, M. B., & Singer, F. J. 1996. Elk population processes in Yellowstone National Park under the policy of natural regulation. *Ecological Applications*, **6**, 573-593.

Creel, S., Winnie, J., Maxwell, B., Hamlin, K., & Creel, M. 2005. Elk alter habitat selection as an antipredator response to wolves. *Ecology*, **86**, 3387-3397.

Chandler, R.B., Engebretsen, K., Cherry, M.J., Garrison, E.P. & Miller, K.V. 2018. Estimating recruitment from capture-recapture data by modelling spatio-temporal variation in birth and age-specific survival rates. *Methods in Ecology and Evolution,* **9,** 2115-2130.

DeCesare, N. J., Hebblewhite, M., Bradley, M., Smith, K. G., Hervieux, D., & Neufeld, L. 2012. Estimating ungulate recruitment and growth rates using age ratios. *The Journal of Wildlife Management*, **76**, 144-153.

DeCesare, N.J., Hebblewhite, M., Lukacs, P.M. & Hervieux, D. 2016. Evaluating Sources of Censoring and Truncation in Telemetry-Based Survival Data. *Journal of Wildlife Management,* **80,** 138-148.

Duquette, J. F., Belant, J. L., Svoboda, N. J., Beyer Jr, D. E., & Albright, C. A. 2014. Comparison of occupancy modeling and radiotelemetry to estimate ungulate population dynamics. *Population Ecology*, **56**, 481-492.

Eberhardt, L. L. 2002. A paradigm for population analysis of long-lived vertebrates. *Ecology*, **83**, 2841-2854.

Ebert, C., Sandrini, J., Spielberger, B., Thiele, B., & Hohmann, U. 2012. Non-invasive genetic approaches for estimation of ungulate population size: a study on roe deer (*Capreolus capreolus*) based on faeces. *Animal Biodiversity and Conservation*, **35**, 267-275.

Escos, J., Alados, C. L., & Emlen, J. M. 1994. Application of the stage-projection model with density-dependent fecundity to the population dynamics of Spanish ibex. *Canadian Journal of Zoology*, **72**, 731-737.

Fisichelli, N. A., Abella, S. R., Peters, M., & Krist Jr, F. J. 2014. Climate, trees, pests, and weeds: Change, uncertainty, and biotic stressors in eastern US national park forests. *Forest Ecology and Management*, **327**, 31-39.

Fiske, I., & Chandler, R. 2011. Unmarked: an R package for fitting hierarchical models of wildlife occurrence and abundance. *Journal of Statistical Software*, 43(10), 1-23.

Gaillard, J. M., Delorme, D., & Jullien, J. M. 1993. Effects of cohort, sex, and birth date on body development of roe deer (*Capreolus capreolus*) fawns. *Oecologia*, **94**, 57-61.

Gaillard, J. M., Festa-Bianchet, M., Yoccoz, N. G., Loison, A., & Toigo, C. 2000. Temporal variation in fitness components and population dynamics of large herbivores. *Annual Review of Ecology and Systematics*, **31**, 367-393.

Grant, K. 2014. Hand-rearing Elk (*Cervus canadensis*).

Greenberg, S., & Godin, T. 2015. A tool supporting the extraction of angling effort data from remote camera images. *Fisheries*, **40**, 276-287.

Griffin, K. A., Hebblewhite, M., Robinson, H. S., Zager, P., Barber-Meyer, S. M., Christianson, D., ... & Johnson, B. K. 2011. Neonatal mortality of elk driven by climate, predator phenology and predator community composition. *Journal of Animal Ecology*, **80**, 1246-1257.

Harris, N. C., Kauffman, M. J., & Mills, L. S. 2008. Inferences about ungulate population dynamics derived from age ratios. *The Journal of Wildlife Management*, **72**, 1143-1151.

Hebblewhite, M., Eacker, D.R., Eggeman, S., Bohm, H. & Merrill, E.H. 2018. Density-Independent Predation Affects Migrants and Residents Equally in a Declining Partially Migratory Elk Population. *Oikos,* **127,** 1304-1318.

Hebblewhite, M., & Merrill, E. H. 2011. Demographic balancing of migrant and resident elk in a partially migratory population through forage–predation tradeoffs. *Oikos*, **120**, 1860-1870.

Hebblewhite, M., Merrill, E.H., & McDermid, G. 2008. A multi-scale test of the forage maturation hypothesis in a partially migratory ungulate population. *Ecological Monographs*, **78**, 141-166.

Hebblewhite, M., Percy, M., & Merrill, E. H. 2007. Are all global positioning system collars created equal? Correcting habitat-induced bias using three brands in the central Canadian Rockies. *The Journal of Wildlife Management*, **71**, 2026-2033.

Hurley, M. A., Unsworth, J. W., Zager, P., Hebblewhite, M., Garton, E. O., Montgomery, D. M., ... & Maycock, C. L. 2011. Demographic response of mule deer to experimental reduction of coyotes and mountain lions in southeastern Idaho. *Wildlife Monographs*, **178**, 1-33.

Ikeda, T., Takahashi, H., Yoshida, T., Igota, H., & Kaji, K. 2013. Evaluation of camera trap surveys for estimation of sika deer herd composition. *Mammal Study*, **38**, 29-34.

Johnson, D.E. 1951. Biology of the elk calf, *Cervus elaphus nelsoni*. *Journal of Wildlife Management,* **15,** 396-410.

Johnson, M. G. .2012. *Tribes of the Sioux Nation*. Bloomsbury Publishing.

MacKenzie, D. I., & Royle, J. A. 2005. Designing occupancy studies: general advice and allocating survey effort. *Journal of Applied Ecology*, **42**, 1105-1114.

MacKenzie, D. I., Nichols, J. D., Lachman, G. B., Droege, S., Andrew Royle, J.A., & Langtimm, C. A. 2002. Estimating site occupancy rates when detection probabilities are less than one. *Ecology*, **83**, 2248-2255.

Majka, D., J. Jenness, and P. Beier. 2007. CorridorDesigner: ArcGIS tools for designing and evaluating corridors. Available at http://corridordesign.org.

Middleton, A. D., Kauffman, M. J., McWhirter, D. E., Jimenez, M. D., Cook, R. C., Cook, J. G., ... & White, P. J. 2013. Linking anti-predator behaviour to prey demography reveals limited risk effects of an actively hunting large carnivore. *Ecology Letters*, **16**, 1023-1030.

Millspaugh, J. J., Washburn, B. E., Milanick, M. A., Beringer, J., Hansen, L. P., & Meyer, T. M. 2002. Non-invasive techniques for stress assessment in white-tailed deer. *Wildlife Society Bulletin*, 899-907.

Moeller, A. K. 2017. New methods to estimate abundance from unmarked populations using remote camera trap data.

Moeller, A.K., Lukacs, P.M. & Horne, J.S. 2018. Three novel methods to estimate abundance of unmarked animals using remote cameras. *Ecosphere,* 9**,** e02331.

Morgantini, L. E., & Hudson, R. J. 1985. Changes in diets of wapiti during a hunting season. *Journal of Range Management*, 77-79.

Morgantini, L. E., & Hudson, R. J. 1989. Nutritional significance of wapiti (*Cervus elaphus*) migrations to alpine ranges in western Alberta, Canada. *Arctic and Alpine Research*, **21,** 288-295.

Nelson, L.J., and J.M. Peek. 1982. Effect of survival and fecundity on rate of increase of elk. Journal of Wildlife Management. 46, 535-540.

Owen-Smith, N., Mason, D. R., & Ogutu, J. O. 2005. Correlates of survival rates for 10 African ungulate populations: density, rainfall and predation. *Journal of Animal Ecology*, **74**, 774-788.

Pojar, T. M., & Bowden, D. C. 2004. Neonatal mule deer fawn survival in west-central Colorado. *The Journal of Wildlife Management*, **68**, 550-560.

Pulliam, H. R., & Danielson, B. J. 1991. Sources, sinks, and habitat selection: a landscape perspective on population dynamics. *The American Naturalist*, **137**, S50-S66.

Raithel, J. D. 2005. Impact of calf survival on elk population dynamics in west-central Montana.

Raithel, J. D., Kauffman, M. J., & Pletscher, D. H. 2007. Impact of spatial and temporal variation in calf survival on the growth of elk populations. *The Journal of Wildlife Management*, **71**,795-803.

Royle, J.A., Chandler, R.B., Sollmann, R. & Gardner, B. 2014. *Spatial capture-recapture,* Academic Press, Elsevier, New York, New York.

Royle, J. A., & Nichols, J. D. 2003. Estimating abundance from repeated presence–absence data or point counts. *Ecology*, **84**, 777-790.

Samuel, M. D., & Garton, E. O. 1994. Horvitz-Thompson survey sample methods for estimating large-scale animal abundance. In *Transactions of the North American Wildlife and Natural Resources Conference*. **59**, 170-179.

Samuel, M. D., Garton, E. O., Schlegel, M. W., & Carson, R. G. 1987. Visibility bias during aerial surveys of elk in northcentral Idaho. *The Journal of Wildlife Management*, 622-630.

Smith, B.L. & McDonald, T. 2002. Criteria to improve age classification of antlerless elk. *Wildlife Society Bulletin,* **30,** 200-207.

Storm, D. J., Samuel, M. D., Van Deelen, T. R., Malcolm, K. D., Rolley, R. E., Frost, N. A., ... & Richards, B. J. 2011. Comparison of visual-based helicopter and fixed-wing forward-looking infrared surveys for counting white-tailed deer *Odocoileus virginianus*. *Wildlife Biology*, **17**, 431-441.

Swift, P. K., Bleich, V. C., Stephenson, T. R., Adams, A. E., Gonzales, B. J., Pierce, B. M., & Marshal, J. P. 2002. Tooth extraction from live-captured mule deer in the absence of chemical immobilization. *Wildlife Society Bulletin*, **30,** 253-255.

Unsworth, J. W., Kuck, L., Garton, E. O., & Butterfield, B. R. 1998. Elk habitat selection on the Clearwater National Forest, Idaho. *The Journal of Wildlife Management*, 1255-1263.

Unsworth, J. W., Kuck, L., Scott, M. D., & Garton, E. O. 1993. Elk mortality in the Clearwater drainage of northcentral Idaho. *The Journal of Wildlife Management*, 495-502.

Unsworth, J. W., Pac, D. F., White, G. C., & Bartmann, R. M. 1999. Mule deer survival in Colorado, Idaho, and Montana. *The Journal of Wildlife Management*, 315-326.

Walsh, N. E., Griffith, B., & McCabe, T. R. 1995. Evaluating growth of the Porcupine Caribou Herd using a stochastic model. *The Journal of Wildlife Management*, 262-272.

Zero, V. H., Sundaresan, S. R., O'Brien, T. G., & Kinnaird, M. F. 2013. Monitoring an endangered savannah ungulate, Grevy's zebra *Equus grevyi*: choosing a method for estimating population densities. *Oryx*, **47**, 410-419.

Appendices

Table A1: Top ($\leq$ 4 ΔAIC) occuRN univariate detection probability models for calf elk incorporating abiotic, biotic, and anthropogenic covariates to best inform influence of detection (*r*) on Abundance estimates (*N*) at the Ya Ha Tinda, Alberta, Canada using *n*=37 cameras. Detection probability was fixed as a constant and tested for effect of top covariate (~1 covariate +1) and is logit transformed, K is the number of parameters in the model.

Detection top (*p) Model	K	SE	AIC	ΔAIC
Early Spring- Period 1				
~1 + ndist_road.s ~ 1	3	1.062	83.530	0
~1 + regen500.s ~ 1	3	1.645	84.624	1.094
~1 + cuts100.s ~ 1	3	1.219	85.792	2.262
~1 + burns500.s ~ 1	3	1.218	85.892	2.362
~1 + dhimin100.s ~ 1	3	0.624	85.897	2.367
~1~ 1 (*null)*	3	0.793	86.649	3.119
Spring – Period 2				
~1 + dhiseas100.s ~ 1	3	0.232	115.922	0
~1 + dhicum100.s ~ 1	3	0.956	117.944	2.022
~1 + NDVIAug20.s ~ 1	3	0.508	119.657	3.735
~1~ 1 (*null)*	2	1.221	126.596	10.674
Summer – Period 3				
~1 + ndist_road.s ~ 1	3	0.529	119.287	0
~1 + dhiseas100.s ~ 1	3	0.549	120.578	1.291
~1 + dhimin100.s ~ 1	3	0.084	120.623	1.336
~1 + regen500.s ~ 1	3	0.720	120.628	1.341
~1 + burns500.s ~ 1	3	0.691	121.423	2.136
~1 ~ 1	2	0.582	121.915	2.628
~1 + dhicum100.s ~ 1	3	0.207	122.503	3.216
~1 + cuts100.s ~ 1	3	0.576	122.707	3.42
Late Summer – Period 4				
~1 + dhicum20.s ~ 1	3	0.682	138.678	0
~1 + dhiseas20.s ~ 1	3	0.992	139.542	0.864
~1 + cuts20.s ~ 1	3	0.394	141.131	2.453
~1 + NDVIJul500.s ~ 1	3	0.348	141.640	2.962
~1 + NDVIAug500.s ~ 1	3	0.345	141.835	3.157
~1 + cuts100.s ~ 1	3	0.303	142.169	3.491
~1 ~ 1	2	0.365	147.129	8.451
Fall – Period 5				
~1 + ndist_edge.s ~ 1	3	0.036	125.0819	0
~1 + dhimin20.s ~ 1	3	0.120	125.178	0.097
~1 + d2road.s ~ 1	3	0.183	126.233	1.151

~1 ~ 1	2	0.006	126.320	1.238
~1 + dhicum20.s ~ 1	3	0.168	126.460	1.378
~1 + dhiseas100.s ~ 1	3	0.184	126.913	1.831
~1 + dhiseas20.s ~ 1	3	0.294	127.315	2.233
~1 + NDVIJul100.s ~ 1	3	0.293	127.368	2.286

Table A2: Top ($\leq$ 4 ΔAIC) occuRN univariate detection probability models for adult female elk incorporating abiotic, biotic, and anthropogenic covariates to best inform influence of detection (*r*) on Abundance estimates (*N*) at the Ya Ha Tinda, Alberta, Canada using *n*=37 cameras. Detection probability was fixed as a constant and tested for effect of top covariate (~1 covariate +1) and is logit transformed, K is the number of parameters in the model.

Detection top (*p) Model	**K**	**SE**	**AIC**	**ΔAIC**
Early Spring- Period 1				
~1 + ndist_road.s ~ 1	3	0.641	197.472	0
~1~ 1 (*null)*	2	0.336	219.994	22.52
Spring – Period 2				
~1 + dhiseas100.s ~ 1	3	0.181	294.588	0
~1 + dhicum100.s ~ 1	3	0.166	296.717	2.129
~1 + NDVIJul20.s ~ 1	3	0.658	297.292	2.704
~1~ 1 (*null)*	2	1.221	303.109	8.521
Summer – Period 3				
~1 + NDVIJul20.s ~ 1	3	0.267	226.632	0
~1 + dhiseas100.s ~ 1	3	0.298	226.679	0.047
~1 + NDVIAug20.s ~ 1	3	0.274	226.766	0.134
~1 + dhimin100.s ~ 1	3	0.497	226.934	0.302
~1 + dhicum100.s ~ 1	3	0.266	226.970	0.338
~1 + ndist_road.s ~ 1	3	0.2917	228.533	1.901
~1 ~ 1 (*null*)	2	0.437	234.378	7.746
Late Summer – Period 4				
~1 + regen20.s ~ 1	3	0.496	259.238	0
~1 + cuts100.s ~ 1	3	0.192	262.077	2.839
~1 + dhimin20.s ~ 1	3	0.211	262.533	3.295
~1 ~ 1 (*null)*	2	0.428	265.706	6.468
Fall – Period 5				
~1 + NDVIAug100.s ~ 1	3	0.188	262.496	0
~1 + NDVIJul100.s ~ 1	3	0.193	262.550	0.054
~1 + NDVIJul500.s ~ 1	3	0.171	262.813	0.317
~1 + NDVIAug500.s ~ 1	3	0.172	262.976	0.48
~1 + regen500.s ~ 1	3	0.865	264.268	1.772
~1 + tpi100.s ~ 1	3	0.148	265.674	3.178
~1 ~ 1 (*null)*	2	1.581	266.523	4.027